

Electronic properties of an ordered-disordered interface

L. G. Parent,* H. Ueba,[†] and S. G. Davison

*Quantum Theory Group, Applied Mathematics Department, University of Waterloo,
Waterloo, Ontario N2L 3G1, Canada*

(Received 28 August 1981)

The coherent potential approximation is extended to an ordered-disordered interface which is composed of a monatomic crystal and a disordered binary material. A proper description of disorder is achieved by performing the self-consistent calculation of the coherent potential after the formation of the interface. These goals are accomplished by a Green's-function method and perturbation theory. A density-of-states calculation is performed and the various kinds of interface states are discussed. The virtual-crystal approximation is utilized to separate interface effects from those of disorder. In particular, disorder affects all interface states in the same qualitative manner, regardless of whether they are associated with the ordered or disordered material. In general, the effect of disorder on interface states is found to be analogous to its effect on the bulk bands.

I. INTRODUCTION

The quantum-mechanical theory of solid-solid interfaces is an expanding branch of surface physics. At present, most models developed correspond to an ideal interface,¹⁻⁹ which is formed by matching two semi-infinite ordered solids having the same translational symmetry parallel to the interface. However, many problems of surface physics resemble more closely an ordered-disordered interface, for example a solid-liquid interface or a solid-alloy interface. Although desirable, a realistic model of a liquid or an alloy will not be developed here. Instead, a simplified model of disorder will be employed to conceptualize the effect that disorder has on the electronic properties of the interface. For such a model, preliminary discussions of the electronic characteristics of simple molten salts have already been reported.^{10,11}

The interface model is constructed by combining established solid-state models: The ordered crystal is represented by a monatomic lattice where the tight-binding approximation is employed, while the disordered material, having two atomic components, is modeled via the coherent potential approximation (CPA).¹²⁻¹⁴ A Green's-function formalism is adopted, so that the electronic properties may be characterized by a density-of-states calculation. The interface Green's function is calculated by considering the formation of the interface as a perturbation on the two semi-infinite materials; this is achieved via the Dyson equation. The semi-infinite Green's function of either material is

derived, from the corresponding bulk Green's function, by a perturbation approach known as the cleavage plane method.¹⁵

Although specific interface effects, such as charge transfer and vacancies,⁶⁻⁹ have been incorporated into three-dimensional models in a self-consistent manner, a simple one-dimensional model will be considered here in order to simplify the solution of the interface problem, since, as will be shown later, disorder on its own introduces self-consistency into the problem in a unique way. Such a one-dimensional model is sufficient because it reflects the amalgamation and persistent behavior of the bulk bands of materials with diagonal disorder, and provides a description of the electronic states that are localized perpendicular to the interface (i.e., localized along the one-dimensional chain). In fact, for three-dimensional systems with translational symmetry parallel to the interface, a mixed Bloch-Wannier representation^{7-9,15} reproduces the flavor of a one-dimensional approach, except that the determination of the Green's function is complicated by the additional bonds occurring in the three-dimensional situation. The main advantage of the simpler model is that it provides a more transparent formalism for the discussion of disorder, while retaining the salient features. Thus, as in the past,¹⁻⁴ the one-dimensional model is utilized for instructive purposes rather than as an earnest attempt to reproduce reality.

The one-dimensional model is limited to the discussion of strongly persistent-type materials, where both the interface and bulk bands are of the per-

sistent-type. In other words, an accurate treatment of amalgamation-type interface states is not possible, since each configuration in the average has a unique atom associated with the interface site. However, insight is provided so that the occurrence of an amalgamation-type interface band may be understood.

The basic formalism is presented in Sec. II, where the bulk and surface properties of each component of the interface are first outlined, then the interface is formulated by coupling the two separate media across their surfaces. In particular, a detailed discussion of the surface states of the disordered material is included, since it provides the insight necessary to unravel the interface problem. The crucial step in modeling the interface is the introduction of the interface coherent potential in a self-consistent manner, so that the effects of disorder are properly taken into account. In Sec. III, the local density of states of the disordered interface site is exploited to characterize the various electronic properties, with special emphasis on the interface states. The conclusions are presented in the last section.

II. MODEL SYSTEM

Throughout, all systems will be represented by the tight-binding Hamiltonian

$$H = \sum_m \epsilon_m |m\rangle \langle m| - \sum_{m \neq m'} J_{mm'} |m\rangle \langle m'|, \quad (1)$$

where ϵ_m is the energy level of the orbital $|m\rangle$ on the m th site and $J_{mm'}$ is the transfer energy between the sites m and m' . The difference between order and disorder, which will be considered here, is characterized by whether ϵ_m takes a fixed value (ordered site) or a random value (disordered site). Thus, Eq. (1) corresponds to an ordered (monatomic) system when every ϵ_m is a fixed value, to a disordered system when every ϵ_m is a random variable, and to an ordered-disordered interface when every ϵ_m on the left of the interface is a fixed value and each ϵ_m on the right is a random variable.

The Green's function is defined by

$$G(E) = (E - H)^{-1}, \quad (2)$$

and may be utilized to characterize the electronic properties of each material via the density of states,

$$\rho(E) = \pi^{-1} \text{Im Tr} G(E) = \sum_m \rho_m(E), \quad (3)$$

where

$$\begin{aligned} \rho_m(E) &= \pi^{-1} \text{Im} \langle m | G(E) | m \rangle \\ &= \pi^{-1} \text{Im} G(E, m, m) \end{aligned} \quad (4)$$

is the local density of states.

Rather than solving the interface Hamiltonian directly, a sequence of perturbation steps will be employed so that the interface Green's function may be determined by the Dyson equation. The preliminary steps involve brief derivations of the bulk and surface properties of each material, while the final step culminates with the Green's-function formulation of the interface. It should be realized that this approach is more general than the one-dimensional situation which follows.

A. Ordered crystal

An ordered monatomic crystal or metal may be represented by an infinite linear chain composed of equally spaced sites which are consecutively numbered. To emphasize the monatomic nature and to prevent confusion with the disordered material to be developed subsequently, the subscript 1 will be used throughout to label quantities associated with an ordered site. The choice $\epsilon_m = \epsilon_1$ for all sites and $J_{mm'} = J_1$ between nearest neighbors in Eq. (1) leads to the bulk energy

$$E(k) = \epsilon_1 - 2J_1 \cos ka_1, \quad (5)$$

where a_1 is the lattice constant. The corresponding infinite Green's function G_1 is given by

$$G_1(E, m, m') = M^{-1} \sum_k \frac{e^{i(m-m')ka_1}}{E - E(k)}. \quad (6)$$

The summation over k may be converted into an integral, so that

$$G_1(E, m, m') = t_1^{|m-m'|} [2s_1 J_1 (\xi_1^2 - 1)^{1/2}]^{-1}, \quad (7)$$

where

$$\begin{aligned} t_1 &= \xi_1 + s_1 (\xi_1^2 - 1)^{1/2}, \\ \xi_1 &= (\epsilon_1 - E) / 2J_1, \end{aligned} \quad (8)$$

and

$$s_1 = \begin{cases} 1, & \xi_1 < -1 \\ -1 & \text{otherwise} \end{cases}. \quad (9)$$

Since $G_1(E, m, m)$ is independent of m , the local density-of-states Eq. (4) turns out to be site indepen-

dent, and is nonzero only in the bulk band region defined by Eq. (5).

A fundamental step towards the formulation of an interface is the formation of a semi-infinite ordered crystal ($m \geq 1$) from the infinite linear chain by the Kalkstein and Soven method.¹⁵ An imaginary cleavage plane is passed through the infinite crystal between the sites $m = 0$ and 1 to form two disconnected systems. The local perturbation

$$v_1 = J_1 |0\rangle\langle 1| + D_1 |1\rangle\langle 1| \quad (10)$$

is introduced to describe the cleavage process on the semi-infinite chain to the right ($m \geq 1$), where the first term eliminates the bond (cleavage plane), while the environmental shift D_1 is also introduced to account for the potential change felt by the electron at the end of the chain (i.e., at the surface atom of the one-dimensional model).

The Dyson equation

$$g_1(E) = G_1(E) + G_1(E)v_1g_1(E) \quad (11)$$

leads to the Green's function of the semi-infinite crystal, viz.,

$$g_1(E, m, m') = G_1(E, m, m') \times [1 + 2t_1^P(D_1 + J_1 t_1)/F_1^s(E)], \quad (12)$$

where

$$p = m + m' - |m - m'| - 2, \quad (13)$$

$$F_1^s(E) = 2J_1 s_1 (\xi_1^2 - 1)^{1/2} - 2D_1 - 2J_1 \xi_1, \quad (14)$$

and, in particular, the surface Green's function is given by

$$g_1^s(E) = g_1(E, 1, 1) = 2/F_1^s(E). \quad (15)$$

At this point, the electronic properties of an ordered crystal with a surface may be described, and one of the semi-infinite formalisms necessary for the formation of the interface, via perturbation theory, is complete.

Since this ordered surface model is the prototype for everything which follows, it warrants a brief description. The local density of states at the surface may be calculated from Eq. (15), and is composed of a bulk band modified by the presence of the surface, and possibly a single δ function located at the surface state energy E_1^s , which is defined by the possible pole of Eq. (15). Such a pole arises whenever

$$|D_1| > J_1 \quad (16)$$

and corresponds to an electronic state that decays along the chain as one moves away from the surface. As shown in the Appendix, these localized states give rise to a local density of states of the form

$$\rho_1^s(E) = I_1^s(E_1^s) \delta(E - E_1^s), \quad (17)$$

where

$$I_1^s(E) = 1 - J_1^2/D_1^2. \quad (18)$$

Thus, this approach is adequate to describe both the localized and bulk states of an ordered surface. The existence condition equation (16) implies that a localized or surface state only occurs when the perturbation is sufficiently large.

These surface-states ideas will be used in later sections to explain the effects that disorder has on surface and interface states. A binary disordered material may be connected to a corresponding ordered material via the virtual-crystal approximation, as will be demonstrated subsequently.

B. Disordered crystal

Before proceeding to a discussion of infinite or semi-infinite disordered materials, a general formulation of the CPA will be presented. Essentially, the disordered material is represented by an effective medium by introducing the coherent potential, which may be calculated in a self-consistent manner. This effective medium plays such a dominant role in the formalism that the subscript eff (and later simply e) will be used extensively to label quantities associated with the disordered material.

This theory may be used to treat binary systems composed of the atoms A and B which are characterized by the atomic energies ϵ_A and ϵ_B and by the concentrations C_A and $C_B (= 1 - C_A)$, respectively. Further, it will be assumed that an electron is allowed to transfer between nearest-neighbor sites with the transfer energy $J_{mm'} = J_{\text{eff}}$, which is taken independent of site occupation. In a disordered system, the exact configuration is not known, so that its properties are determined by averaging over all the allowed configurations. In the present case, Eq. (1) represents the Hamiltonian of an allowed configuration, where ϵ_m is a random atomic level ϵ_A or ϵ_B , depending on whether an atom A or B occupies the site m . These types of systems are said to have diagonal disorder or randomness.

The Hamiltonian of an allowed configuration may be written as

$$H_{\text{con}} = H_{\text{vir}} + \Delta \sum_m N_m |m\rangle \langle m|, \quad (19)$$

where

$$H_{\text{vir}} = \epsilon_{\text{vir}} \sum_m |m\rangle \langle m| - J_{\text{eff}} \sum_{m \neq m'} |m\rangle \langle m'|, \quad (20)$$

is an ordered (monatomic) Hamiltonian which describes a virtual crystal with a mean atomic energy $\epsilon_{\text{vir}} = C_A \epsilon_A + C_B \epsilon_B$, $\Delta = \epsilon_A - \epsilon_B$ is the difference in atomic energies of the disordered material, and N_m is a random variable which takes the value C_B at an A atom and $-C_A$ at a B atom. In other words, N_m converts the virtual crystal into the corresponding configuration. The randomness of the system is characterized by introducing the ensemble-averaged Green's function,

$$G_{\text{eff}}(E) = \langle G_{\text{con}}(E) \rangle_{\text{av}}, \quad (21)$$

which is used to describe the properties of the disordered system. The crucial step in the CPA is that G_{eff} is used to define an effective medium by introducing the effective Hamiltonian H_{eff} which is defined by

$$G_{\text{eff}}(E) = (E - H_{\text{eff}})^{-1}. \quad (22)$$

The effective Hamiltonian describes the averaged crystal and has the form

$$H_{\text{eff}} = H_{\text{vir}} + \sum_m \sigma_m(E) |m\rangle \langle m|, \quad (23)$$

where σ_m is the coherent potential of the m th site which represents the shift and the broadening of the states of the virtual crystal. As is well known, the effective medium described by the coherent potential is determined by setting the averaged scattering potential $\langle t_m \rangle_{\text{av}} (= C_A t_A + C_B t_B)$ of a single site immersed in the medium equal to zero. This condition leads to a self-consistent equation which determines the coherent potential,¹³ namely,

$$\sigma_m = (\Delta C_B - \sigma_m) G_{\text{eff}}(E, m, m) (\Delta C_A + \sigma_m). \quad (24)$$

Once σ_m is determined as a function of energy, the electronic properties of the disordered system may be described by a density-of-states calculation with the aid of Eqs. (22) and (23).

In principle, Eq. (24) is applicable to any system with diagonal disorder, whether it is infinite, finite, one dimensional, or three dimensional; the practical difficulty is calculating G_{eff} . Moreover, Eq. (24) contains implicit as well as explicit self-consistency; the former arises due to the fact that G_{eff} depends on σ_m as seen from Eqs. (22) and (23). In

the remainder of this section, these ideas will be demonstrated for the bulk and semi-infinite systems. Then the results will be extended to the interface situation in the next section.

To emphasize the one-dimensional nature of the following calculations, all three letter subscripts, such as eff , will be shortened to their first letter. For convenience, all energies will be measured in units of $2J_e$, ϵ_B will be taken as the energy zero, and C will denote the concentration of atom A , so that

$$\begin{aligned} J_e &= \frac{1}{2}, \quad \epsilon_B = 0, \quad \epsilon_A = \Delta, \\ C &= C_A, \quad C_B = 1 - C, \end{aligned} \quad (25)$$

and the disordered material is specified by C and Δ .

Equation (23) shows that the coherent potential may be interpreted as a perturbation which transforms the ordered virtual crystal into the effective medium. Thus, one may obtain G_{eff} by modifying the Green's function of the virtual crystal. In fact, for the bulk situation, the Green's function of the effective medium may be obtained directly from the Green's function of the ordered crystal given in Eq. (7), by the conversion

$$G_e(E, m, m') = G_1(E + \epsilon_1 - C\Delta - \sigma_m, m, m'). \quad (26)$$

In this case, $G_e(E, m, m)$ is independent of m , and Eq. (24) reduces to a single equation which determines the bulk coherent potential $\sigma_b (= \sigma_m$ for all m) of the infinite system. As a result, the effective Hamiltonian possesses the full translational symmetry of the virtual crystal and, conceptually, H_e may be thought of as the Hamiltonian of an effective periodic medium. The conversion of an ordered Green's function to the effective Green's function outlined in Eq. (26) is obvious, from a perturbation point of view, when σ_m is independent of m , and very useful. However, care must be taken when generalizing this procedure to the semi-infinite case, as will be shown later.

The conversion Eq. (26) leads to the bulk Green's function of the effective medium given by

$$G_e(E, m, m') = t_e^{|m-m'|} [s_e(\zeta_e^2 - 1)^{1/2}]^{-1}, \quad (27)$$

where

$$\begin{aligned} t_e &= \zeta_e + s_e(\zeta_e^2 - 1)^{1/2}, \\ \zeta_e &= C\Delta + \sigma_b - E, \end{aligned} \quad (28)$$

and

$$s_e = \pm 1 \text{ such that } |t_e| < 1. \quad (29)$$

Unlike the ordered case, from which it is derived, s_e cannot be easily specified, since ζ_e depends on the yet unknown σ_b . Thus, the self-consistent equation (24) is rewritten as

$$2[E - (1-C)\Delta]\sigma_b^3 + [\Delta^2(5C^2 - 6C + 1) + 2C\Delta E - E^2 + 1]\sigma_b^2 + 2\Delta^3 C(1-C)(1-2C)\sigma_b + \Delta^4 C^2(1-C)^2 = 0. \quad (30)$$

This cubic has three real roots, or one real and two complex, as functions of E , C , and Δ . The correct root must satisfy the original equation (24) before squaring to obtain Eq. (30), and may be described as a continuous function of E , except possibly for a pole at $E = \Delta(1-C)$ in a region where $\sigma_b^I = \text{Im}\sigma_b = 0$, with the property that $\sigma_b^I \geq 0$. Since $G_e(E, m, m)$ is independent of m , the local density of states is the same for all sites, and is nonzero in the energy regions where $\sigma_b^I > 0$. As far as the bulk situation is concerned, it is sufficient to solve Eq. (30) in the energy regions where there are one real and two complex roots, and the correct root satisfies $\sigma_b^I > 0$. However, in the semi-infinite and interface situations it will be necessary to choose the correct solutions for the other case when there are three real roots. Fortunately, the procedure given above works in both cases.

With the bulk coherent potential determined, the local density of states may be calculated from $G_e(E)$, and the resulting band structure may be of two types depending on C and Δ . The first (persistence) type retains the individual characteristics

of the two constituent atoms; the second (amalgamation) type combines the features of the components. In other words, the binary disordered material may have a two-band or a single-band structure. Moreover, the one-dimensional model presented here reflects qualitatively both possibilities for these types of materials.

The site-diagonal Green's function for a semi-infinite disordered system depends on the site m which, via Eq. (24), leads to the site-dependent coherent potential. This can be seen by attempting to include the implicit dependence of σ_m in Eq. (12), as was accomplished for the bulk situation in Eq. (26). However, such a converted semi-infinite Green's function does not properly take into account the site dependence of σ_m required by Eq. (24). In general, the Green's function must include a diagonal perturbation on each site, so that the site dependence of σ_m may be treated in the correct manner. Thus, care must be taken in this situation.

The complications of the semi-infinite system have been reported by Ueba and Ichimura,^{16,17} who incorporated them into a model by restricting the site dependence of σ_m to the surface atom, and introduced the surface coherent potential σ_s , while using the bulk coherent potential σ_b on the remaining sites.

By replacing the diagonal perturbation D_1 of the surface atom by $D_e + \sigma_s - \sigma_b$ and E by $E + \epsilon_1 - C\Delta - \sigma_b$ in Eq. (12), the site dependence of the coherent potential in their model is properly included, and the semi-infinite Green's function is given by

$$g_e(E, m, m') = G_e(E, m, m') \{ 1 + t_e^p [2(D_e + \sigma_s - \sigma_b) + t_e] / F_e^s(E) \}, \quad (31)$$

where

$$F_e^s(E) = s_e (\zeta_e^2 - 1)^{1/2} - 2(D_e + \sigma_s - \sigma_b) - \zeta_e. \quad (32)$$

In particular, the surface Green's function is expressed as

$$g_e^s(E) = g_e(E, 1, 1) = 2 / F_e^s(E). \quad (33)$$

Within this simplified model, the self-consistent equation (24) corresponds to two coupled equations which determine σ_s and σ_b , namely,

$$\sigma_s = [\Delta(1-C) - \sigma_s] g_e^s(E) (\Delta C + \sigma_s), \quad m = 1 \quad (34)$$

and

$$\sigma_b = [\Delta(1-C) - \sigma_b] G_e(E, m, m) (\Delta C + \sigma_b), \quad m > 1. \quad (35)$$

With the aid of Eqs. (28), (32), and (33), Eq. (34) is rewritten as

$$\sigma_s(E) = 2\Delta^2 C(1-C) [s_e (\zeta_e^2 - 1)^{1/2} - 2\Delta(1-2C) - 2D_e + \sigma_b + E - C\Delta]^{-1}, \quad (36)$$

so that the surface coherent potential is isolated.

The local density of states at the surface is then calculated from Eq. (33) and is composed of a band structure analogous to that of the bulk together with possibly two surface states.¹⁷ This band structure is defined by the energy regions where $\sigma_s^I > 0$, and it can be shown that

$$\sigma_s^I(E) > 0 \text{ whenever } \sigma_b^I(E) > 0, \quad \sigma_s^I(E) = 0 \text{ whenever } \sigma_b^I(E) = 0. \quad (37)$$

Consequently, the band-structure type at the surface is the same as that of the bulk. In addition, a surface state may appear whose energy E_e^s lies outside the band structure (determined by poles of g_e^s), and whose density of states is given by

$$\rho_e^s(E) = I_e^s(E_e^s) \delta(E - E_e^s), \quad (38)$$

where

$$I_e^s(E) = 2 \{ [1 + s_e \zeta_e (\zeta_e^2 - 1)^{-1/2}] (\sigma_b' - 1) - 2(\sigma_s' - 1) \}^{-1}, \quad (39)$$

is the intensity of the surface state and the prime indicates differentiation with respect to E .

By comparison of Eqs. (18) and (39), it is obvious that disorder has modified the properties of the surface states. Within the virtual-crystal approximation, the disordered system reduces to an ordered one with $\epsilon_1 = c\Delta$, $J_1 = J_e = \frac{1}{2}$, and $D_1 = D_e$, which is easily verified by setting $\sigma_b = \sigma_s = 0$. The intensity equation (39) and the virtual-crystal approximation may be exploited to distinguish between the effects that disorder and surface formation have on the properties of the surface states.

The local density of states at the surface is shown in Fig. 1, where, as will be explained later (Fig. 3), not one, but two surface states exist below the amalgamation bulk band. As Δ increases, the

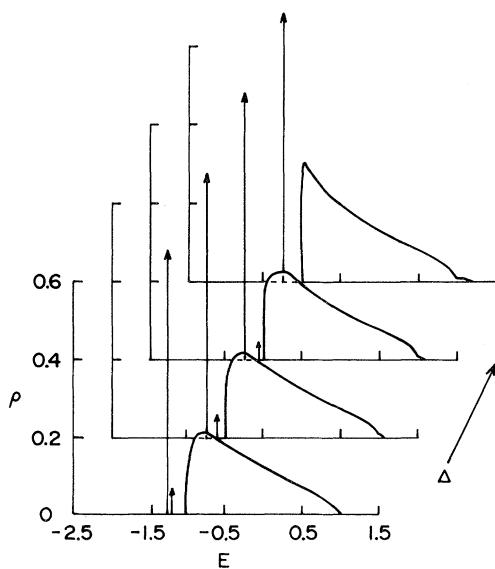


FIG. 1. Local density of states at a disordered surface for $D_e = -1$, $C = 0.1$, and $\Delta = 0.1, 0.2, 0.3$, and 0.4 .

separation of these states widens, until one enters the bulk band, while the other remains relatively insensitive to changes in Δ . The surface-state intensities reflect the concentrations of each atom in the sense that the surface state with the higher energy has the smaller intensity and the atom with the higher electronic energy level $\epsilon_A (= \Delta)$ has the lower concentration $C_A (= C)$. These ideas are clarified in Fig. 2, where $I_e^s(E_e^s)$ is plotted against concentration for a persistent-type case. Here, the dramatic effect of concentration on the surface-state intensities is clearly demonstrated, since $I_e^s(E_e^s)$ varies between zero and $I_v^s(E_v^s) = 0.75$, the

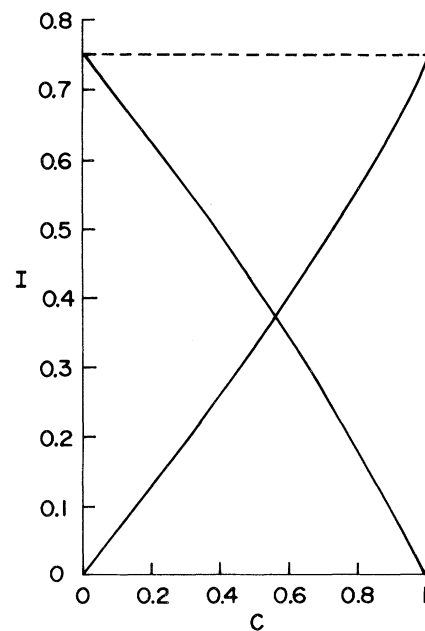


FIG. 2. Surface state intensities vs concentration for $\Delta = 2$, and $D_e = -1$. Solid line is I_e^s of disordered system, broken line is I_v^s of virtual crystal.

virtual-crystal approximation value for $0 \leq C \leq 1$. As C increases, $I_e^s(E_e^s)$ of the lower E_e^s decreases almost linearly between the extremes, while the intensity of the surface state with the upper E_e^s value increases.

Concentration effects on E_e^s are portrayed in Fig. 3, where two surface states exist and the bulk bands (shaded areas) are of the persistent type. The surface-state energy levels E_e^s vary only slightly with concentration and tend to follow the bulk band edge directly above each of them. In the virtual-crystal approximation, the surface-state energy,

$$E_v^s = C\Delta + D_e + \frac{1}{4D_e}, \quad |D_e| > \frac{1}{2} \quad (40)$$

is a linear function of C , which connects the opposite ends of the disordered levels. The effect of disorder and surface formation on E_e^s may be separated by a simple interpretation of the Z pattern formed by the E_e^s 's and E_v^s . The formation of the surface creates a surface state with energy E_v^s when disorder is neglected. On introducing disorder, the single-level E_v^s is split into two levels, one being above and the other below E_v^s . The magnitude of the surface-state splitting is governed by Δ and is only slightly affected by C . It should be noted that Fig. 3 shows that the surface state, which vanishes in Fig. 1, reappears between the bands for sufficiently large Δ .

The preceding evidence allows each surface state

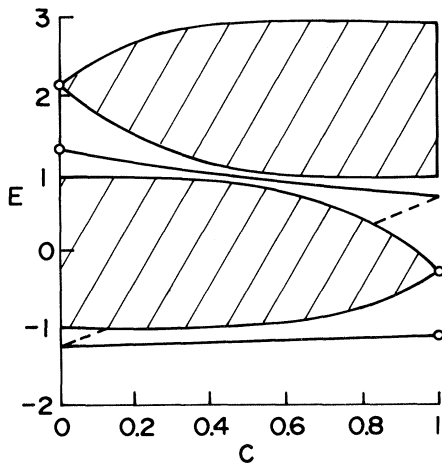


FIG. 3. Surface state energies vs concentration for $\Delta=2$ and $D_e=-1$. Solid line is E_e^s of disordered system, broken line is E_v^s of the virtual crystal. Circles denote limit points which arise in monatomic cases. Shaded areas are disordered bulk bands.

to be identified with a particular component atom. The lower E_e^s value corresponds to the atom with the smaller energy level; the upper E_e^s level is identified with the other atom whose energy level is the higher one. Physically, this is a natural association since the surface site may be occupied by either atom whose effect on the surface state properties (E_e^s, I_e^s) will be different. Indeed, the influence of each atom on I_e^s is weighted by the occupational probability, or concentration, at the surface, while the sensitivity of E_e^s is amplified by the magnitude of Δ . These ideas also apply to the single surface-state case. However, here identification is more difficult, but may be achieved by observing how I_e^s varies with concentration. For persistent materials, each bulk band corresponds to an atom, so a surface state may be linked directly to a band. This description of surface states lays the foundation for the discussion of the interface states.

C. Interface formation

The crucial step in describing an ordered-disordered interface is the extension of the CPA to such a situation. The effective medium in this case corresponds to an interface composed of an ordered crystal (averaging unnecessary) and an effective disordered medium (averaging accounted for by coherent potential) whose associated Green's function will be denoted by G^i . Intuitively, the desired extension is achieved when G_{eff} is replaced by G^i in the self-consistent equation (24). In so doing, the coherent potential, and hence the electronic properties, of each disordered site is calculated within the interface environment in which it resides. In other words, the coherent potential will be calculated after the formation of the interface; it will be determined by the interface Green's function G^i , not the semi-infinite Green's function. This amounts to a new interface effect, which is unique to the ordered-disordered interface. In the next section, this approach will be physically justified when the coherent potential is discussed in detail.

In general, the diagonal elements of the interface Green's function are site dependent, which leads to a site-dependent coherent potential as in the semi-infinite system. Following the semi-infinite model of Ueba and Ichimura, the site dependence of the coherent potential will be restricted to the disordered site adjacent to the interface by introducing the interface coherent potential σ_i at this site. A perturbation approach may then be used to calcu-

late G^i by coupling the semi-infinite materials together. The interface coherent potential may be calculated self-consistently and the electronic properties characterized by a density-of-states calculation.

This approach is analogous to the semi-infinite model. However, to emphasize the difference, the surface coherent potential σ_s is replaced by the interface coherent potential σ_i , since, as will be shown later, these quantities are indeed different. The interface model is illustrated in Fig. 4, where γ denotes the interface coupling between the materials. The interface Green's function is calculated by the Dyson equation

$$G^i(E) = g^i(E) + g^i(E)VG^i(E), \quad (41)$$

$$G^i(E, m, m') = g^i(E, m, m') + \gamma [g^i(E, m, 0)G^i(E, 1, m') + g^i(E, m, 1)G^i(E, 0, m')], \quad (44)$$

where

$$G^i(E, 0, m') = [g^i(E, 0, m') + \gamma g^i(E, 0, 0)g^i(E, 1, m')]/d, \quad (45)$$

$$G^i(E, 1, m') = [g^i(E, 1, m') + \gamma g^i(E, 1, 1)g^i(E, 0, m')]/d, \quad (46)$$

and

$$d = 1 - \gamma^2 g^i(E, 0, 0)g^i(E, 1, 1). \quad (47)$$

The disordered interface site is characterized by

$$G_e^i(E) = G^i(E, 1, 1) = 2/F_e^i(E), \quad (48)$$

where

$$F_e^i(E) = s_e(\zeta_e^2 - 1)^{1/2} - 2[\Gamma_e(E) + \sigma_i - \sigma_b] - \zeta_e, \quad (49)$$

and

$$\Gamma_e(E) = D_e + 2\gamma^2/[2J_1s_1(\zeta_1^2 - 1)^{1/2} - 2D_1 - 2J_1\zeta_1], \quad (50)$$

while the ordered interface site is described by

$$G_1^i(E) = G^i(E, 0, 0) = 2/F_1^i(E), \quad (51)$$

where

$$F_1^i(E) = 2J_1s_1(\zeta_1^2 - 1)^{1/2} - 2\Gamma_1(E) - 2J_1\zeta_1, \quad (52)$$

and

$$\Gamma_1(E) = D_1 + 2\gamma^2/[s_e(\zeta_e^2 - 1)^{1/2} - 2(D_e + \sigma_i - \sigma_b) - \zeta_e]. \quad (53)$$

where $g^i(E)$ is the Green's function of the disconnected semi-infinite systems ($\gamma=0$) given by

$$g^i(E, m, m') = \begin{cases} g_1(E, 1-m, 1-m'), & m, m' < 1 \\ g_e(E, m, m'), & m, m' > 0 \\ 0, & \text{otherwise} \end{cases} \quad (42)$$

and

$$V = \gamma(|0\rangle\langle 1| + |1\rangle\langle 0|) \quad (43)$$

is the perturbation potential which unites the two systems.

In a straightforward manner, the interface Green's function is given by

Since the diagonal element $G^i(E, m, m)$ of the interface Green's function depends on the site, due to the semi-infinite Green's functions, the inclusion of the site-dependent coherent potential is dictated by the extension of the self-consistent equation (24), while restriction of it to the interface site is reasonable in the tight-binding approximation. With the aid of Eqs. (24), (28), and (48), the interface coherent potential is given by

$$\sigma_i(E) = 2\Delta^2 C(1-C)[s_e(\zeta_e^2 - 1)^{1/2} - 2\Delta(1-2C) - 2\Gamma_e + \sigma_b + E - C\Delta]^{-1}. \quad (54)$$

It can be shown that

$$\begin{aligned} \sigma_i^I(E) &> 0 \text{ whenever } \sigma_b^I(E) \text{ or } \Gamma_e^I(E) > 0 \\ \sigma_i^{(E)} &= 0 \text{ whenever } \sigma_b^I(E) \text{ and } \Gamma_e^I(E) = 0, \end{aligned} \quad (55)$$

so that, when $\gamma \neq 0$, the local density of states of

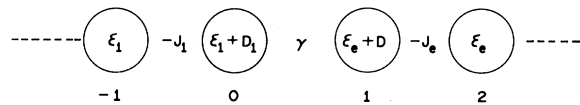


FIG. 4. Ordered-disordered interface model, where $\epsilon_e = C\Delta + \sigma_b$, $D = D_e + \sigma_i(E) - \sigma_b(E)$, and γ is the interface coupling.

the disordered interface site is nonzero for energies which lie in the bulk bands of either material. In other words, the band structures of the materials are blended when they are in electrical contact. It should be noted that σ_i reduces to σ_s of Eq. (36) when $\gamma=0$, as expected. However, for $\gamma \neq 0$, σ_i deviates from σ_s due to the interface effects contained within $\Gamma_e(E)$. These results will be graphically illustrated shortly.

With σ_b and σ_i completely specified, the electronic properties of the disordered interface site may be characterized by the local density of states given by

$$\rho_e^i(E) = \pi^{-1} \text{Im} G_e^i(E) = \pi^{-1} \text{Im} G^i(E, 1, 1), \quad (56)$$

which will be referred to as simply the disordered density of states. Analogous to the semi-infinite situation, this density of states is composed of a modified bulk structure together with interface states. The energies E^i of these interface states are determined by the poles of Eq. (48), which are given by

$$E^i = C\Delta + \Gamma_e + \sigma_i + [4(\Gamma_e + \sigma_i - \sigma_b)]^{-1}, \quad (57)$$

subject to the existence condition

$$|\Gamma_e + \sigma_i - \sigma_b| > \frac{1}{2}. \quad (58)$$

As detailed in the Appendix, the disordered density of states reduces to

$$\rho_e^i(E) = I_e^i(E^i) \delta(E - E^i), \quad (59)$$

in the vicinity of E^i , where

$$I_e^i(E) = 2 \{ [1 + s_e \zeta_e (\zeta_e^2 - 1)^{-1/2}] (\sigma_b' - 1) - 2(\Gamma_e' + \sigma_1' - 1) \}^{-1}, \quad (60)$$

is the intensity on the disordered interface site.

In a similar manner, the ordered density of states

$$\rho_1^i(E) = \pi^{-1} \text{Im} G_1^i(E) = \pi^{-1} \text{Im} G^i(E, 0, 0) \quad (61)$$

is associated with the ordered interface site, the poles of Eq. (51) being defined by

$$E^i = \epsilon_1 + \Gamma_1 + J_1^2 / \Gamma_1, \quad (62)$$

subject to the existence condition

$$|\Gamma_1(E^i)| > J_1. \quad (63)$$

In the vicinity of E^i , the ordered density of states is given by

$$\rho_1^i(E) = I_1^i(E^i) \delta(E - E^i), \quad (64)$$

where

$$I_1^i(E^i) = 2[1 - s_1 \zeta_1 (\zeta_1^2 - 1)^{-1/2} - 2\Gamma_1']^{-1} \quad (65)$$

is the intensity at the ordered interface site.

It should be realized that Eqs. (57) and (62) are equivalent when $\gamma \neq 0$, since the zeros of Eqs. (49) and (52), and hence the poles of the Green's functions equations (48) and (51), are identical, in spite of the fact that this conclusion is obscured by the squaring procedure used to derive these results.

For completeness, both these results have been included to establish the parallelism between the different sites, and because both semi-infinite results can be obtained directly. Moreover, Eqs. (57) and (62) are in fact self-consistent equations, since σ_i , σ_b , Γ_e , and Γ_1 are all evaluated at E^i .

The virtual-crystal approximation corresponds to an ordered-ordered interface, which may be specified by setting $\sigma_b = \sigma_i = \sigma_b' = \sigma_i' = 0$ in the previous results. As in the semi-infinite case, the intensity equation (60) and the virtual-crystal approximation will be exploited to differentiate the effects that disorder and interface formations have on the properties of the interface states. This discussion will lead to the conclusion that the effect of disorder on interface states is analogous to its effect on the bulk bands.

III. INTERFACE ELECTRONIC STRUCTURE

The interface electronic structure bears evidence of the constituent materials whose characteristics manifest themselves in a density-of-states calculation. A detailed analysis of the disordered density of states reveals the features which may be anticipated in the present situation. However, since the coherent potential plays a fundamental role in the description of the electronic properties of disordered materials, it is appropriate to begin the discussion with it.

A. Interface coherent potential

The imaginary parts of the bulk, surface, and interface coherent potentials, calculated from Eqs. (30), (36), and (54), respectively, are compared in Fig. 5. The interface effects, incorporated self-consistently into the interface coherent potential, are revealed by comparison with the others. In the energy regions, where σ_b^I and σ_s^I are nonzero, σ_i^I is also nonzero. However, σ_i^I is nonzero in the region

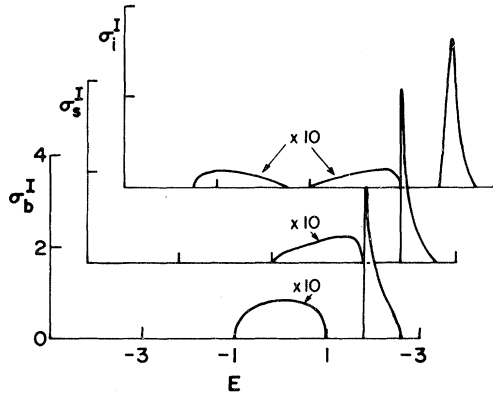


FIG. 5. Imaginary parts of the bulk, surface, and interface coherent potentials for $C=0.1$ and $\Delta=2.0$.

of the ordered material's bulk band as well. Moreover, the three quantities may be viewed as a sequence of events which introduce modification at each step. This demonstrates the need to incorporate site dependence into the coherent potential.

The significance of the interface effects contained in σ_i may be demonstrated by determining the circumstances under which σ_i reduces to σ_b . With the aid of Eq. (27), Eqs. (35) and (54) lead to

$$\sigma_i - \sigma_b = \frac{1}{2} \sigma_i [s_e(\zeta_e^2 - 1)^{1/2} + 2\Gamma_e + \zeta_e] \times [s_e(\zeta_e^2 - 1)^{1/2} + \sigma_b - (1 - 2C)\Delta]^{-1}, \quad (66)$$

so that

$$\sigma_i = \sigma_b, \quad (67)$$

whenever

$$\Gamma_e(E) = \frac{1}{2} [s_e(\zeta_e^2 - 1)^{1/2} - \zeta_e]^{-1}. \quad (68)$$

Equation (68) has been written in a form which is directly comparable to Eq. (50) and shows, by comparison, that Eq. (67) holds whenever

$$D_1 = D_e = 0, \quad s_1 = s_e, \quad \zeta_1 = \zeta_e, \quad (69)$$

and

$$\gamma = J_1 = J_e = \frac{1}{2}.$$

The conditions (69) are analogous to the conversion of the ordered Green's functions to the disordered one, as specified in the bulk situation by Eq. (26). Physically, the conditions (69) correspond to converting the ordered crystal into an identical disordered system by introducing the bulk coherent potential at each site, thereby reducing the interface to the bulk situation, and hence the interface

coherent potential to the corresponding bulk value. Although interfaces between two disordered materials are beyond this present article, this brief discussion serves as a physical justification of the inclusion of interface effects in the interface coherent potential. The presence of these interface effects differentiates the surface and interface coherent potential. Moreover, Eq. (66) verifies, for a general ordered-disordered interface, that the bulk, surface ($\gamma=0$) and interface coherent potentials are expected to be different from each other, as depicted in Fig. 5.

B. Density of states

In general, an interface involves three types of electronic states,^{2,7,8} the first two of which are associated with the bulk bands of the constituent materials. The first type of state has an energy level that lies in the bulk bands of both materials; the second type has an energy level that lies in the bulk band of only one material, and these states decay inside the other material. The third type or interface state decays in both directions perpendicular to the interface and has an energy level outside the bulk bands of both media. Being divorced from their bulk counterpart, interface states are of special interest.

Each type of state is reflected differently in the local density of states. The decaying portion of a state is characterized by a local density of states whose value, for the corresponding energy, vanishes as one moves away from the interface, while a part of a state associated with a bulk band gives rise to a nonzero value at large distances from the interface. The three types of states correspond to the possible combinations of these two characterizations. For convenience, the discussion of states identified with bulk bands will focus on the second kind; this may be achieved by ensuring that the bulk bands of the materials do not overlap each other. Moreover, although interface states will be mentioned near the end of this section, the details will be postponed until the following section.

From a point of view of bulk states and disorder, the quantities of greatest interest are γ , Δ , and C . The general effect of the interface coupling γ on the disordered density of states is illustrated in Fig. 6, where the disordered material is of the persistent type. As γ increases, the area under the density of states grows in the region of the ordered band and shrinks in the disordered bands. This shift of area agrees with the fact that integration

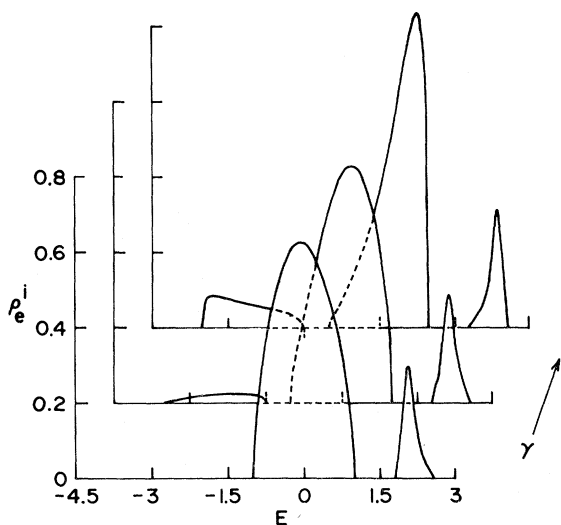


FIG. 6. Disordered density of states for $C=0.1$, $\Delta=2.0$, $D_e=D_1=0$, $\epsilon_1=-2.5$, $J_1=0.5$, and $\gamma=0, 0.5$, and 1.0 . Ordered band lies below the disordered bands.

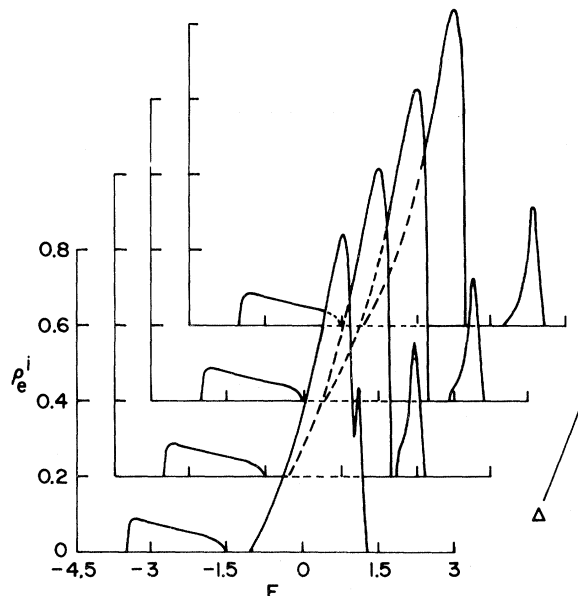


FIG. 7. Disordered density of states for $\epsilon_1=-2.5$, $J_1=0.5$, $D_1=D_e=0$, $\gamma=1.0$, $C=0.1$, and $\Delta=0.5, 1.0, 1.5$, and 2.0 .

of a local density of states yields unity in the present model. Physically, the presence of the ordered band on the disordered interface site is due to the interaction across the interface, and corresponds to the decaying portions of the ordered bulk states which penetrate the disordered material.

The energy difference Δ of the disordered material affects the density of states through its disordered components. This is demonstrated in Fig. 7, where again the ordered band lies below the disordered one. On increasing Δ , the disordered band is transformed from the amalgamation type to the persistent type, while the ordered component remains the same as long as γ is fixed.

A similar effect can be found by changing the concentration C . For the persistent case, each band associated with the disordered material is identified with a particular atom (of the disordered material) through the observation of its change with concentration. In fact, the upper band is associated with the atoms with the higher electronic energy and the lower band corresponds to the atoms with lower energy. Moreover, the area of these disordered bands reflects the corresponding concentrations, in the sense that they vary together. These trends are visually verified in Fig. 8, where the area of the upper band increases with its concentration.

To this point, the discussion has been restricted to the case of the second kind, so that the various

effects could be studied in isolation. However, the effects of γ , C , and Δ on states of the first kind would be combinations of those previously discussed, thereby obscuring their individuality.

The two types of states associated with the bulk bands are easily understood, because they behave in a similar manner to the band to which they are linked. This is not true for the third type or interface states, since they are localized at the interface

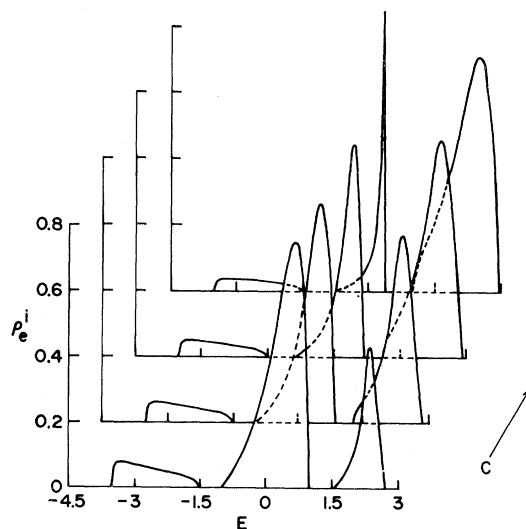


FIG. 8. Disordered density of states for $\epsilon_1=-2.5$, $J_1=0.5$, $D_1=D_e=0$, $\gamma=1.0$, $\Delta=2.0$, and $C=0.2, 0.4, 0.6$, and 0.8 .

with energies outside the bulk bands. When γ is sufficiently large, interface states appear, as shown in Fig. 9. It should be observed that as many as four localized or interface states are found, and the position of the two upper states shift to the higher side, while the others shift to the lower side, when γ increases.

C. Interface states

Although the description of interface states is more complicated than that of the other types, it may be accomplished by analogy with the semi-infinite situation. In the present case, the localized or interface states may be further classified into three distinct classes according to their parentage. The first type, or true interface state, is induced by the formation of the interface and cannot be identified with a surface state of either separated material ($\gamma=0$). The second type, or ordered interface state, corresponds to a modified surface state of the ordered surface; the third type, or disordered interface state, may be identified with a surface state of the corresponding disordered material.

The virtual-crystal approximation is employed to divorce interface effects from those of disorder. The interface state energy level E_v^i of the virtual crystal is given by

$$E_v^i = C\Delta + \Gamma_e(E_v^i) + [4\Gamma_e(E_v^i)]^{-1}, \tag{70}$$

whenever

$$|\Gamma_e(E_v^i)| > \frac{1}{2}. \tag{71}$$

These results are obtained by eliminating σ_i and σ_b in Eqs. (57) and (58), i.e., by removing the quantities which characterize the disorder. The virtual-crystal approximation leads to an ordered-ordered interface in which a maximum of two interface states have been found.^{2,8}

The effect of the interface coupling γ on the true interface states is illustrated in Fig. 10, where their energy levels E_t^i and those of the virtual crystal are presented. In general, each virtual energy level E_v^i is "sandwiched" between two E_t^i levels, thereby defining distinct groups of levels whose interpretations enable the effects of disorder and interface coupling to be understood. The qualitative effect of γ on the energy levels is easily visualized by the group structures, i.e., the lower group decreases with increasing γ , while the upper one increases. Within each group, the lower E_t^i level is identified with the atom of the disordered material whose

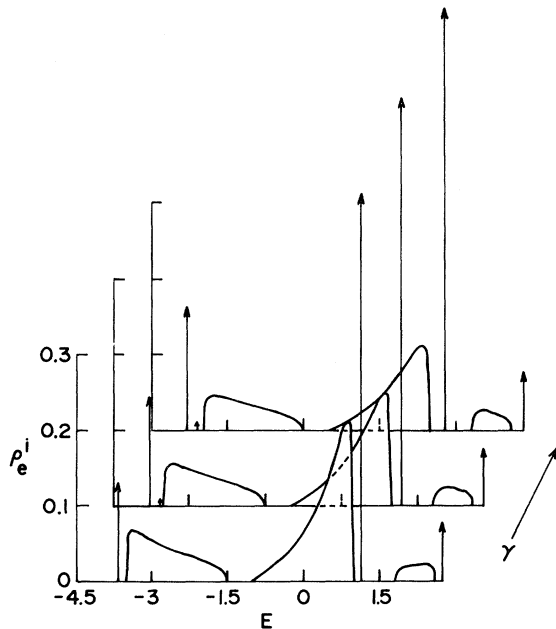


FIG. 9. Disordered density of states for $C=0.1$, $\Delta=2.0$, $D_e=D_1=0$, $\epsilon_1=-2.5$, $J_1=0.5$, and $\gamma=1.7$, 1.8 , and 1.9 .

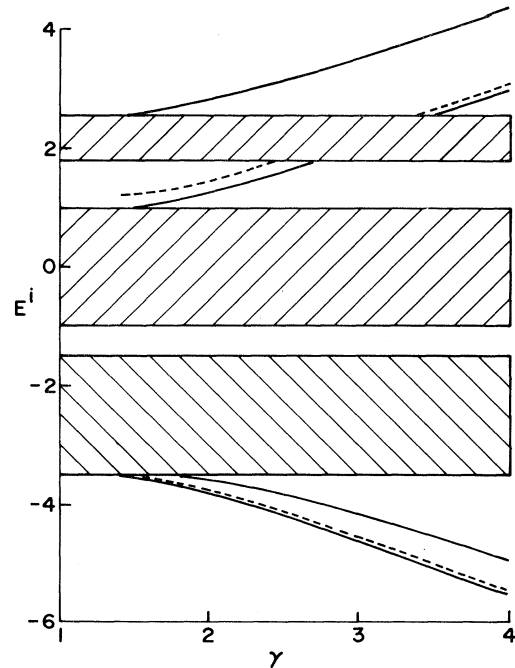


FIG. 10. True interface state energies vs interface coupling for $C=0.1$, $\Delta=2.0$, $D_e=D_1=0$, $\epsilon_1=-2.5$, and $J_1=0.5$. Solid and broken lines correspond to E_t^i and E_v^i of the disordered and virtual systems, respectively. Ordered band lies below the disordered ones. The bands are represented by the different shaded areas.

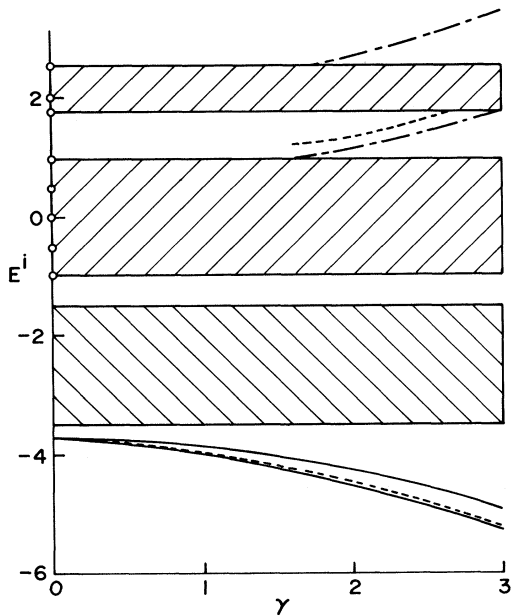


FIG. 11. Ordered interface state energies vs interface coupling for $C=0.1$, $\Delta=2.0$, $D_e=0$, $\epsilon_1=-2.5$, $J_1=0.5$, and $D_1=-1.0$. The solid and equally broken lines correspond to E_e^i and E_v^i , respectively, while the unequally broken line is E_t^i .

atomic energy is the smaller, and the upper E_t^i level is associated with the other atom. In this case, the E_v^i level of the virtual-crystal approximation represents the effect of interface formation without the influence of disorder. The introduction of disorder splits each E_v^i into the two E_t^i levels, thus giving the group structure a simple physical interpretation, which is reminiscent of the semi-infinite situation. The lower group originates from the ordered band, and is identified with this material, while the upper group corresponds to the disordered medium. Moreover, the group which is associated with the ordered band is influenced more by γ than the other group, since the degree of its splitting increases more noticeably with γ . This is understandable, because the interface coupling strength is a measure of the amount of disorder which is introduced into the ordered system. In fact, this last observation is a manifestation of the interface effects incorporated into the self-consistent calculation of the interface coherent potential.

The interface coupling affects E_1^i and E_e^i , the energies of the ordered and disordered interface states, in a similar manner, as seen from Figs. 11 and 12. As before, the interface state levels and those of the virtual crystal form natural groups whose interpretation explains the effects of disorder

and interface coupling. Thus, each type of interface state is affected in the same qualitative manner. However, the advantages of classifying the interface states are that insight into their origin is provided and that specific effects associated with either material may be examined. In particular, Fig. 11 clearly demonstrates that interface states associated with the ordered material (ordered interface states in this case) have energy levels which separate noticeably as γ increases. This evidence reinforces the corresponding remarks made with regards to Fig. 10. Finally, it should be observed that a second group of true interface states also appears in each diagram when γ is sufficiently large.

The effect of the concentration C on the energy spectrum is typified by Fig. 13, where two true interface states and one disordered interface state exist for all concentrations, the disordered material being of the persistent type. The energy levels of the interface states are relatively insensitive to changes in concentrations. Furthermore, the true interface states and the virtual-crystal level form the familiar Z pattern first encountered in the semi-infinite situation (Fig. 3). However, the Z pattern of the disordered interface states is obscured by the bulk bands. The true interface states are identified with the atoms of the disordered material according to the usual energy relationship,

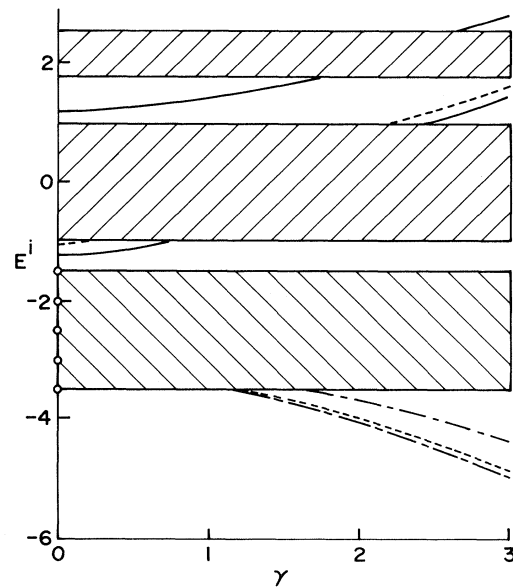


FIG. 12. Disordered interface state energies vs interface coupling for $C=0.1$, $\Delta=2.0$, $\epsilon_1=-2.5$, $J_1=0.5$, $D_1=0$, and $D_e=-1.0$. The solid and equally broken lines correspond to E_e^i and E_v^i , respectively; the unequally broken line is E_t^i .

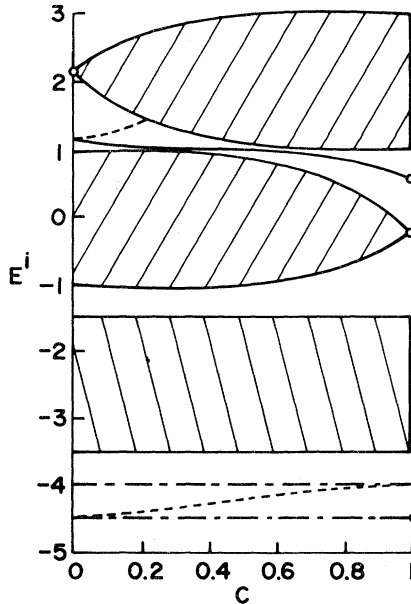


FIG. 13. Disordered interface state energies vs concentration for $\Delta=2.0$, $\epsilon_1=-2.5$, $J_1=0.5$, $D_1=0$, $D_e=-1$, and $\gamma=2.5$. The solid and equally broken lines correspond to E_e^i and E_v^i , respectively; the unequally broken line is E_t^i .

i.e., the state with the lower energy is identified with the atom whose electronic energy is the smaller, while the state with the higher energy is associated with the other atom. The disordered interface state generates the lower portion of the Z pattern and, accordingly, may be identified with the atom of the disordered material which has the lower atomic energy.

The concentration dependence of the intensity of the disordered interface state (Fig. 14) verifies the above identification, since this intensity decreases from that of the virtual crystal to zero as the concentration C of the other atom increases from zero to unity. The intensity of interface states plays an essential role in establishing the connection between these states and the component atoms of the disordered material. In general, the intensities of all interface states reflect the concentrations of the associated atoms of the disordered medium, in the sense that they vary together. In addition, these intensities depend on the interface coupling, as seen from Eqs. (50), (53), (60), and (65).

As in the semi-infinite case, the Z pattern may be interpreted as distinguishing interface effects from those of disorder, since the interface states of the virtual crystal, which correspond only to an interfacial phenomena, are split into two by disorder.

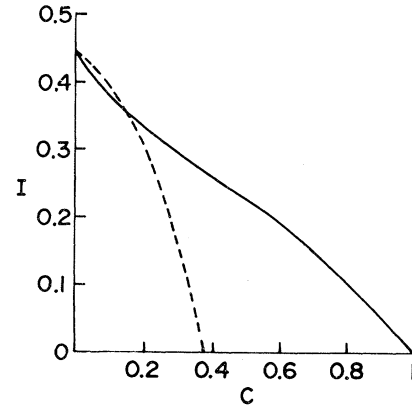


FIG. 14. Intensity of a disordered interface state vs concentration for $\Delta=2.0$, $D_e=-1.0$, $\gamma=2.5$, $\epsilon_1=-2.5$, $J_1=0.5$, and $D_1=0$. Solid and broken lines correspond to E_e^i and E_v^i of the disordered and virtual systems, respectively.

By Eqs. (50) and (70), it can be seen that the amount of splitting is governed by the energy difference Δ of the disordered medium and the interface coupling γ , since E_v^i for $C=0$ and 1 define the corners of the Z pattern and approximate the height of this pattern, so that these particular E_v^i values govern the degree of splitting.

The preceding evidence demonstrates that disorder affects interface states in an analogous manner to its effect on the persistent-type bands of the disordered material. Each interface state and each band is identified with an atomic component of the disordered material. The corresponding intensities reflect that the concentrations and the degree of splitting is essentially governed by the atomic energy difference of the disordered material. Of course, this type of analogy applies to the semi-infinite situation as well.

IV. RESULTS AND DISCUSSIONS

The CPA has been extended to an ordered-disordered interface. The usual perturbation technique used to form an interface from two semi-infinite systems is implemented in a manner which incorporates a proper description of disorder. This is accomplished by the self-consistent calculation of the coherent potential after the formation of the interface, rather than before. As a result, the interface, surface, and bulk coherent potentials are dis-

tinct quantities. The first two being different from the bulk one due to their site dependence, while the interface coherent potential contains interface effects which differentiate it from the corresponding surface value. These interface effects are unique to the ordered-disordered interface.

The separation of interface effects from those of disorder is achieved with the aid of the virtual-crystal approximation which contains only interface effects. In particular, the effect of disorder on interface states is found to be analogous to its effect on the persistent-type bands of the disordered material. Each interface state and each band is identified with a particular atom of the disordered material. In either situation, this identification may be verified by observing the manner in which the intensities vary with concentrations. In other words, the splitting of the interface states of the virtual crystal by disorder is similar to the band splitting induced in a persistent-type material. However, in addition to the energy difference Δ , the interface coupling γ determines the separation of the interface states. In fact, the interface coupling has more pronounced effect on interface states which originate in the ordered material. This is understandable, since the coupling is a measure of the disorder that is introduced into the ordered system. This last observation is a manifestation of the interface effects incorporated into the self-consistent calculation of the interface coherent potential.

A very interesting result of the present model is that disorder splits the interface states regardless of their origin, i.e., whether they are associated with the ordered or disordered material. This is natural, since the interface states are isolated in a one-dimensional model without any associated bandwidth. However, it does imply, for example, that the ordered surface states are expected to split when the ordered system is strenuously coupled to a strongly persistent-type alloy (i.e., large γ and Δ).

Although the one-dimensional model cannot give an accurate treatment of amalgamation-type interface states, it does provide the insight necessary to understand when this situation may arise. The model is easily extended to a three-dimensional one with translational symmetry parallel to the interface. In this case, the coherent potential depends on crystal planes and is the same for every site within each plane. A mixed Bloch-Wannier representation reproduces the flavor of the one-dimensional model, so that the essence of the simpler calculation parallels that of the three-dimensional one. In such an extension, the inter-

face states broaden into bands, which could form an amalgamation band when the splitting of the one-dimensional interface states is sufficiently small. Thus, in general, the effect of disorder on interface states is expected to be analogous to its effect on the bulk bands.

Recently, the surface-state energy levels of a disordered system have been observed¹⁸ as a function of concentration. The material was of the amalgamation type, and only a single surface state was detected for all concentrations. However, the energy of this state could not be determined precisely, since the surface-state structure of the real crystal overlapped the bulk band. At this stage of development, it seems reasonable to assume that the surface-state bands will reflect the properties of the bulk bands. Moreover, it should be possible to observe the surface-state splitting found in the one-dimensional treatment described here in the case of strong persistent-type alloys (i.e., large Δ).

As the study of disordered materials develops, it should be possible to observe that the effect of disorder on interface states is analogous to its effects on the bulk bands, as found in the present one-dimensional model. In particular, disorder affects interface states regardless of their origin, i.e., whether they originate from the ordered or disordered material.

ACKNOWLEDGMENTS

One of us (L.G.P.) would like to express his deep appreciation to R. Barrie and R. Parsons for their patience and encouragement during the writing of this paper. This work was supported by the National Science and Engineering Research Council of Canada.

APPENDIX: INTENSITY OF INTERFACE STATES

Since the intensity of interface states plays a fundamental role in understanding the effects of disorder on the properties of these states, a derivation of this intensity at the disordered interface site will be presented. The corresponding intensities at ordered and disordered surface sites or at the ordered interface site may be derived in a similar manner.

The disordered interface site is characterized by

$$G_e^i(E) = 2/F_e^i(E) . \quad (A1)$$

The intensities of interface states may be determined by a Taylor approximation of $F_e^i(E)$ about $E = E_0$, i.e.,

$$F_e^i(E) \simeq F_e^i(E_0) + 2(E - E_0)/I_e^i(E_0), \quad (\text{A2})$$

where

$$I_e^i(E) = 2/[F_e^i(E)]', \quad (\text{A3})$$

the prime denoting differentiation with respect to E . By Eq. (49), the quantity which will subsequently be shown to be the desired intensity is given by

$$I_e^i(E) = 2\{ [1 + s_e \zeta_e (\zeta_e^2 - 1)^{-1/2}] (\sigma_b' - 1) - 2(\Gamma_e' + \sigma_1' - 1) \}^{-1}. \quad (\text{A4})$$

Consequently, it follows that

$$G_e^i(E) \simeq I_e^i(E_0) \left[\frac{1}{2} I_e^i(E_0) F_e^i(E_0) + (E - E_0) \right]^{-1}. \quad (\text{A5})$$

Moreover, the energy E^i of an interface state is determined by the poles of Eq. (A1), i.e.,

$$F_e^i(E^i) = 0. \quad (\text{A6})$$

As a result, replacing E_0 and E by E^i and $E - i\delta$ in Eq. (A5) leads to

$$G_e^i(E - i\delta) \simeq I_e^i(E^i) \left[\frac{(E - E^i) + i\delta}{(E - E^i)^2 + \delta^2} \right], \quad (\text{A7})$$

and

$$\rho_e^i(E) = \pi^{-1} \text{Im} G_e^i(E) = I_e^i(E^i) \delta(E - E^i), \quad (\text{A8})$$

in the vicinity of E^i .

*Present address: Department of Physics, University of British Columbia, Vancouver, British Columbia V6T 1W5 Canada.

†Permanent address: Department of Electronics, Toyama University, Takaoka, Toyama, Japan.

¹E. Aerts, *Physica* **26**, 1047 (1960).

²S. G. Davison and Y. C. Cheng, *Int. J. Quantum Chem. Symp.* **2**, 303 (1968).

³E. N. Foo and H. S. Wong, *Phys. Rev. B* **10**, 4819 (1974).

⁴E. N. Foo and S. G. Davison, *Surf. Sci.* **55**, 274 (1976).

⁵S. G. Louie and M. L. Cohen, *Phys. Rev. B* **13**, 2461 (1976).

⁶L. Dobrzynski, S. L. Cunningham, and W. H. Weinberg, *Surf. Sci.* **61**, 550 (1976).

⁷D. N. Lowy and A. Madhukar, *Phys. Rev. B* **17**, 3832 (1978).

⁸A. Yaniv, *Phys. Rev. B* **17**, 3904 (1978).

⁹A. Yaniv, *Phys. Rev. B* **22**, 4776 (1980).

¹⁰S. G. Davison, H. Ueba, and W. R. Fawcett, *J. Electroanal. Chem.* **101**, 109 (1979).

¹¹L. G. Parent, S. G. Davison, and H. Ueba, *J. Electroanal. Chem.* **113**, 51 (1980).

¹²P. Soven, *Phys. Rev.* **156**, 809 (1967).

¹³B. Velický, S. Kirkpatrick, and H. Ehrenreich, *Phys. Rev.* **175**, 747 (1968).

¹⁴Y. Onodera and Y. Toyozawa, *J. Phys. Soc. Jpn.* **24**, 341 (1968).

¹⁵D. Kalkstein and P. Soven, *Surf. Sci.* **26**, 85 (1971).

¹⁶H. Ueba and S. Ichimura, *J. Chem. Phys.* **70**, 1745 (1979).

¹⁷L. G. Parent, H. Ueba, and S. G. Davison, *Phys. Lett.* **78A**, 474 (1980).

¹⁸Y. Tokura, T. Koda, and I. Nakada, *J. Phys. Soc. Jpn.* **47**, 1936 (1979).